SAND2014-2292C

SNL Behavior Modeling — Research path & planned LH2 Experiments

Isaac Ekoto
Ethan Hecht
Chris San Marchi

Sandia National Laboratories is a multi-program laboratory managed and operated by Sandia Corporation, a wholly owned subsidiary of Lockheed Martin Corporation, for the U.S. Department of Energy's National Nuclear Security Administration under contract DE-AC04-94AL85000. SAND NO. 2011-XXXXP

Approach: Use high-fidelity data to develop & validate simplified models that augment quantitative risk modeling.

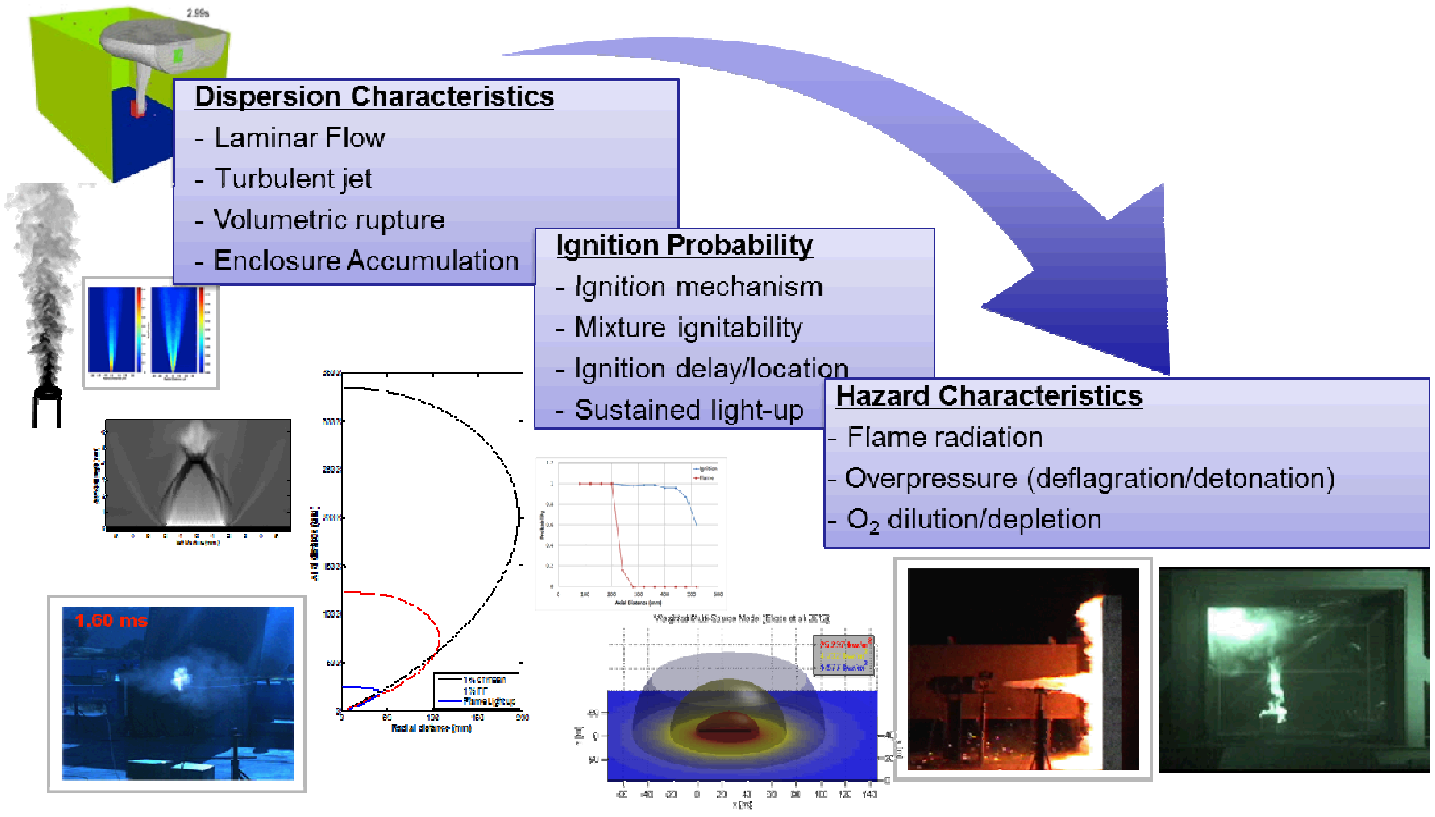

$$Risk \propto \sum_{i,j,k} P(\text{Release}_i) P\left(\text{Ignition}_j | \text{Release}_i\right) P\left(\text{Hazard}_k | \text{Ignition}_j \cap \text{Release}_i\right) P(\text{Harm} | \text{Hazard}_k)$$

Terms in red obtained from physical behavior models, while terms in black are based on scenario frequencies and probit harm models.

FY14 Accomplishment: Overpressure model development

$$\Delta p = p_0 \left\{ \left[\frac{V_T + V_{H2}}{V_T} \frac{V_T + V_{stoich}(\sigma - 1)}{V_T} \right]^{\gamma} - 1 \right\}$$

Bauwens & Dorofeev, ICHS, 2013.

p_0:	Ambient pressure
V_T:	Facility volume
V_{H2}:	Expanded volume of pure H2
V_{stoich}:	Stoichiometric consumed H2 volume
σ:	Stoichiometric H2 expansion ratio
γ:	Air specific heat ratio (1.4)

H2 indoor refueling experiments & modeling

Ekoto et al. IJHE 2012

Houf et al. IJHE 2013

SNL H2 Jet/Plume Model

Houf & Schefer, IJHE 2008

SNL Network Flow Model (NETFLOW)

Winters, SAND 2001-8422

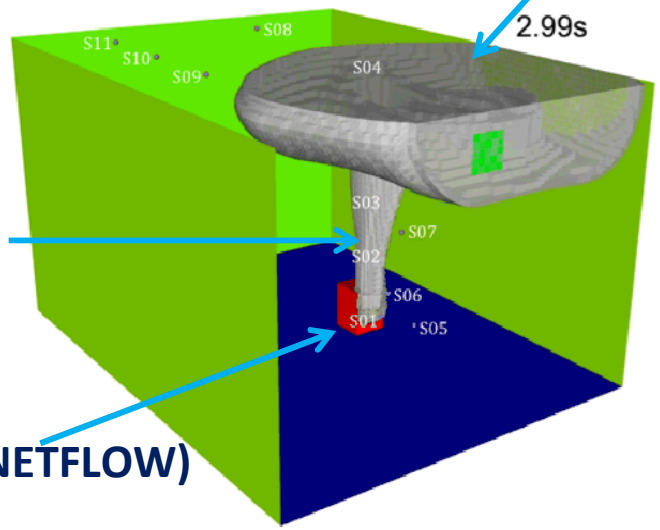

H2 Layer Accumulation Model

Lowesmith et al. IJHE 2009

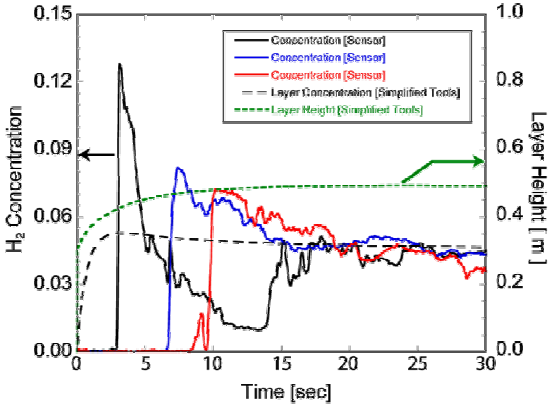

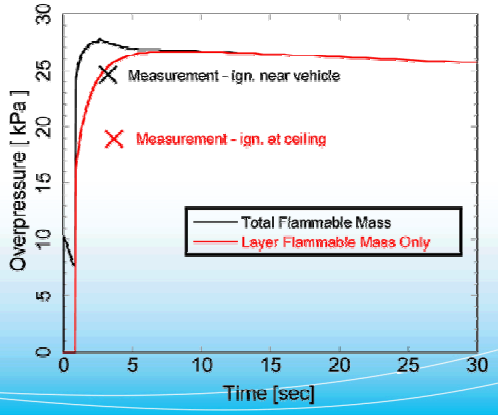

Exercise demonstrates how previous reduced-order model development work can be leveraged to quickly & accurately predict complex behavior.

Economic analyses for a proposed CA network of 68 H2 fuel stations suggests LH2 has long-term benefit over GH2.

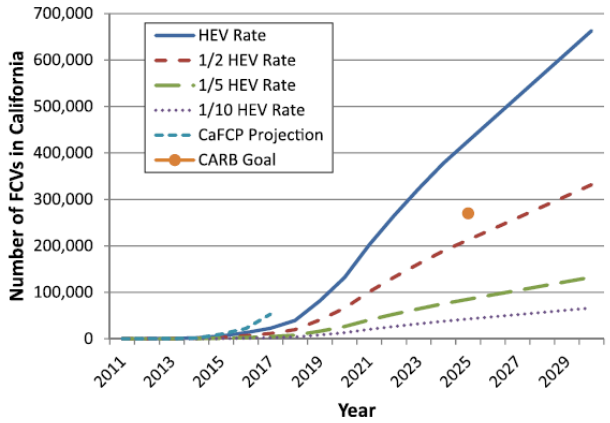

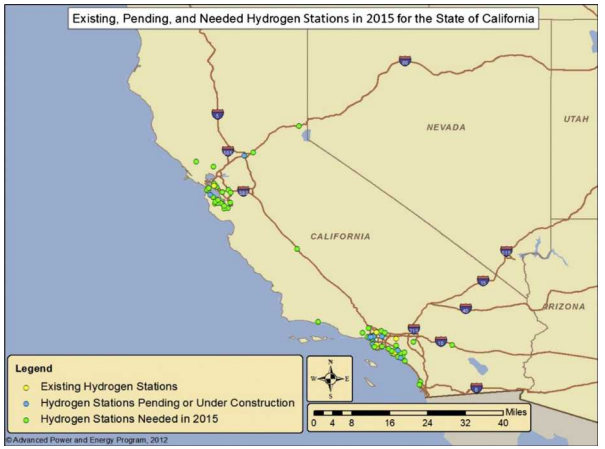

Brown et al., IJHE, 2013

	Total financial support required [$MM]	Total potential profit [$MM]	Weighted average cots of H2 [2011 $/kg]	Onset of positive cash flow [year]	Total H2 dispensed [MMkg]	ROSP
LH2 Only						
100% of Historic HEV Sales	42.7	**543.1**	**6.81**	2017	**155**	11.72
50% of Historic HEV Sales	60.3	**488.0**	**7.16**	2018	**141**	7.09
20% of Historic HEV Sales	84.2	**366.6**	**8.07**	2019	**112**	3.35
10% of Historic HEV Sales	106.1	**168.1**	**10.73**	2021	**67**	0.58
GH2 Only						
100% of Historic HEV Sales	28.0	**230.5**	**8.13**	2016	**87**	7.23
50% of Historic HEV Sales	39.8	**205.2**	**8.57**	2018	**79**	4.16
20% of Historic HEV Sales	56.8	**164.2**	**9.45**	2019	**66**	1.89
10% of Historic HEV Sales	70.0	**132.4**	**10.39**	2020	**57**	0.89

Analysis does not consider feasibility based on safety requirements.

Survey of California Energy Commission preferred stations suggest LH2 separation distances would be prohibitive.

Separation Distances (NFPA 2-2011) **and Areas required for two station concepts**
(critical distances and areas emphasized)

Fueling System Description GH2: 12,500psi storage, 100kg, 0.4"ID tubing with a barrier wall LH2: 3500-15000 gallon (910-1300kg) with barrier wall and insulation	GH2	LH2
Lot lines (ft)	**24**	**33**
Public Streets, Alleys (ft)	24	33
Parking (public assembly) (ft)	13	**75**
Buildings (sprinkled, fire rated) (ft)	10	5
Building Openings or air intakes (ft)	**24**	**75**
Flammable and Combustible liquid storage, vents or fill ports (ft)	10	50
Parking from fill connections on bulk storage (ft)	13	25
Class 1 Div. 2 area diameter (ft)	15	15
Max Bulk Storage Dimensions with Sep. Distances (ft)	78	123
Min Bulk Storage Dimension with Sep. Distances (ft)	68	123
Max Bulk Storage Equipment Dimension with lot lines (ft)	54	40
Min Bulk Storage Equipment Dimension with lot lines (ft)	49	40
Reference Bulk Storage Equipment Area with lot lines (sqft)	2646	1600
Reference Storage Area with Sep. Distances (sqft)	**5304**	**15129**
Note: Add 5 feet for vehicle protection on vehicle facing sides of equipment		

Harris, SAND-2014-XXXX

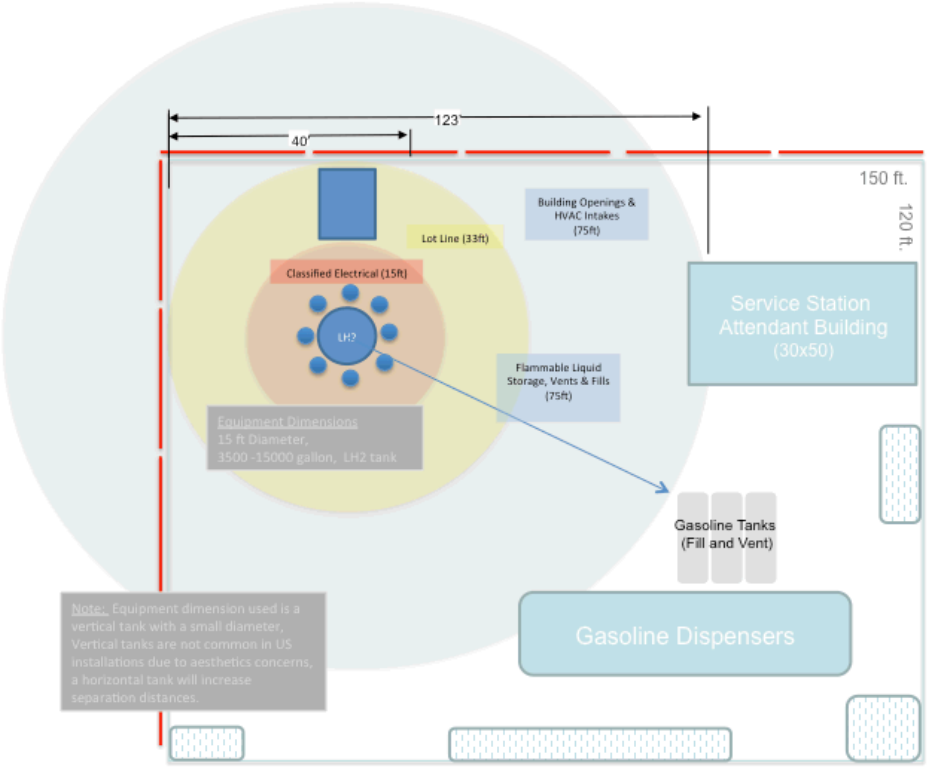

Of 70 stations surveyed (out of 343), none met the NFPA 2 Ch. 6 separation distance requirements.

Improved LH2 modeling needed to reduce separation distances and increase the viability of risk informed certification (e.g., NFPA 2 Ch. 5).

SNL conceptual model for LH2 releases has already been developed – FY09

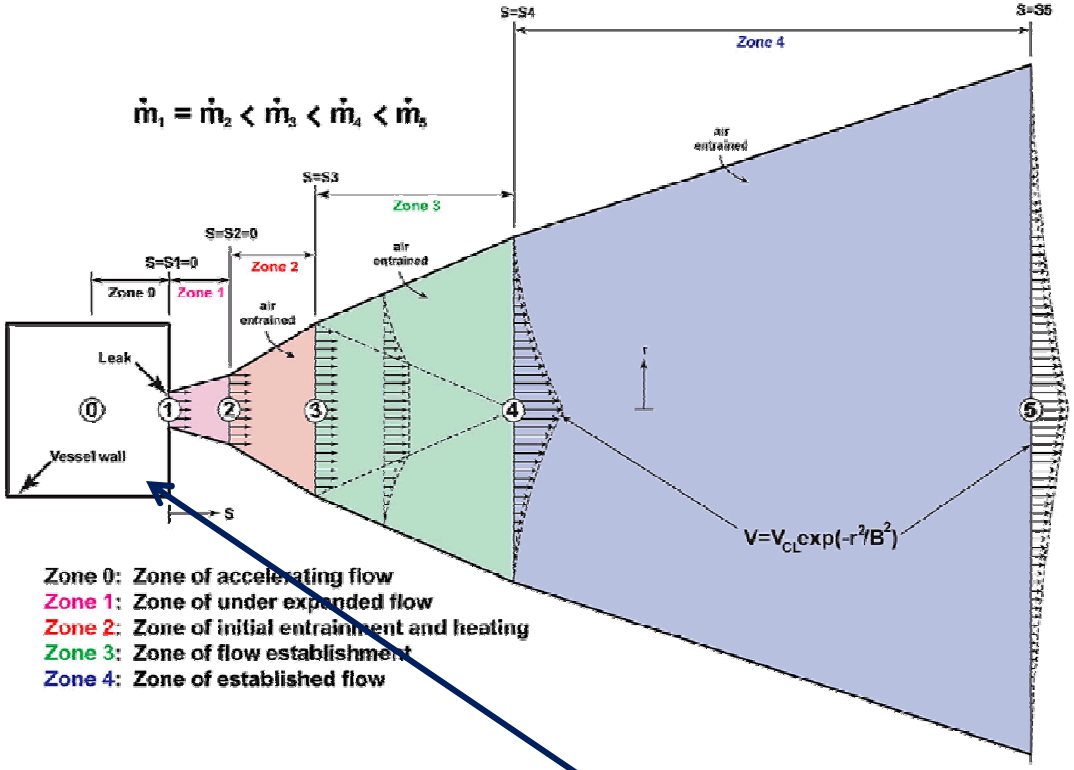

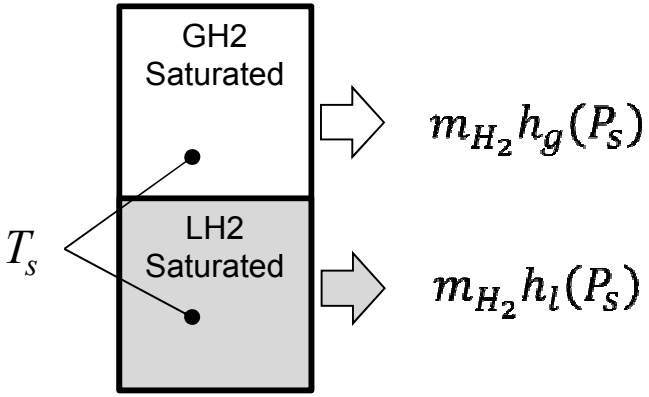

Zone 0 modeled assuming saturation storage conditions and conserved enthalpy from the gas or liquid space.

Winters, SAND 2001-8422

Winters, SAND Report 2009-0035
Winters & Houf, IJHE, 2011
Houf & Winters, IJHE, 2013

SNL Network Flow Analysis Code (NETFLOW) used to model internal conditions in piping, valve, and tanks.

Pseudo source models are used to account for choked flow behavior (Zone 1).

Several source models have been developed to predict the mass weighted effective diameter, (i.e., the critical scaling parameter): $d^* \equiv d_{eff}\sqrt{\rho_{eff}/\rho_{amb}}$

Ruggles & Ekoto, *IJHE*, 2012

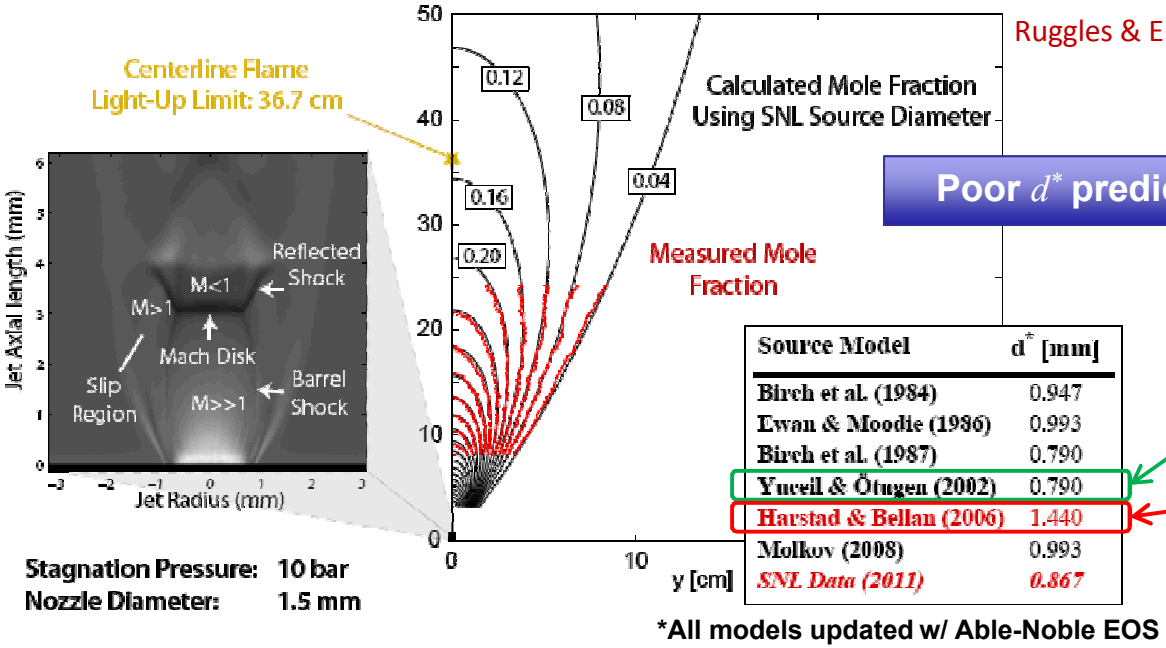

Source Model	d* [mm]
Birch et al. (1984)	0.947
Ewan & Moodie (1986)	0.993
Birch et al. (1987)	0.790
Yuceil & Ötugen (2002)	0.790
Harstad & Bellan (2006)	1.440
Molkov (2008)	0.993
SNL Data (2011)	*0.867*

*All models updated w/ Able-Noble EOS

Poor d^* prediction

Neglects Mach Disk (i.e., fully supersonic) **SNL preferred model**

Assumes ***all*** flow goes through Mach disk (i.e., fully subsonic)

Reality is that fluid is split between the slip and Mach disk regions

Two-zone source model that accounts for the fluid split ratio between the slip region & Mach disk region is needed.

Plug flow assumption invoked for Zone 2.

unknowns
assumed value

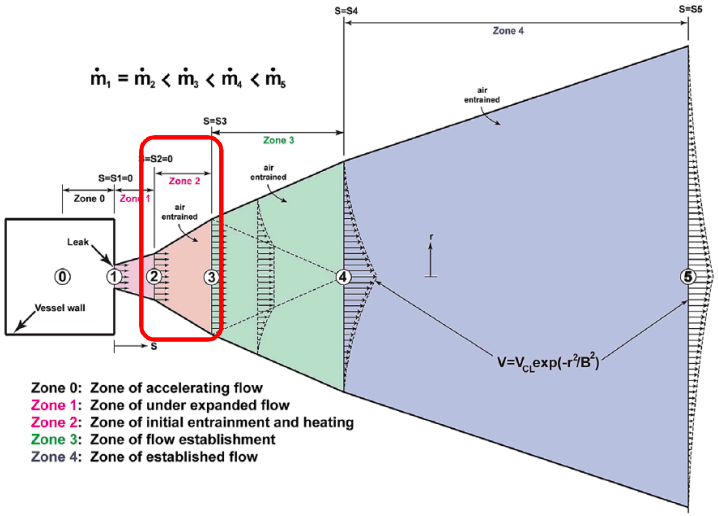

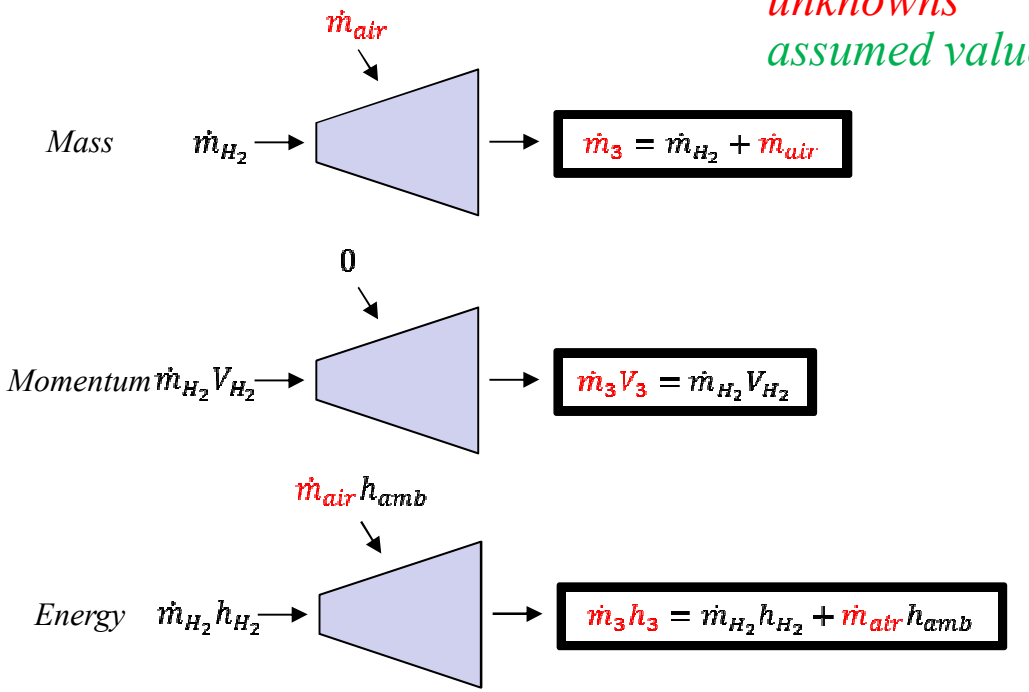

Winters, SAND Report 2009-0035

State modeling by NIST H_2 EOS: $h_3 = f(Y_{H_2,3}, p_{amb}, T_3)$

Species conservation used to close system of equations:

$$\dot{m}_{air} = \dot{m}_{H_2} \frac{1 - Y_{H_2,3}}{Y_{H_2,3}}$$

Turbulent jet entrainment rate used to estimate zone length:

$$E_{mom} \equiv \frac{1}{\rho_{amb}} \frac{d\dot{m}}{dS} \approx \frac{1}{\rho_{amb}} \frac{\dot{m}_{air}}{S_3} \Rightarrow S_3 = \frac{\dot{m}_{air}}{E_{mom} \rho_{amb}}, \text{ where } E_{mom} = \alpha_m \left(\frac{\pi D_{H_2}^2}{4} \frac{\rho_{H_2} V_{H_2}^2}{\rho_{amb}} \right)^{\frac{1}{2}}$$

Zone 3 treated as discrete region w/ boundary conditions specified from self-similar profiles at Zone 4.

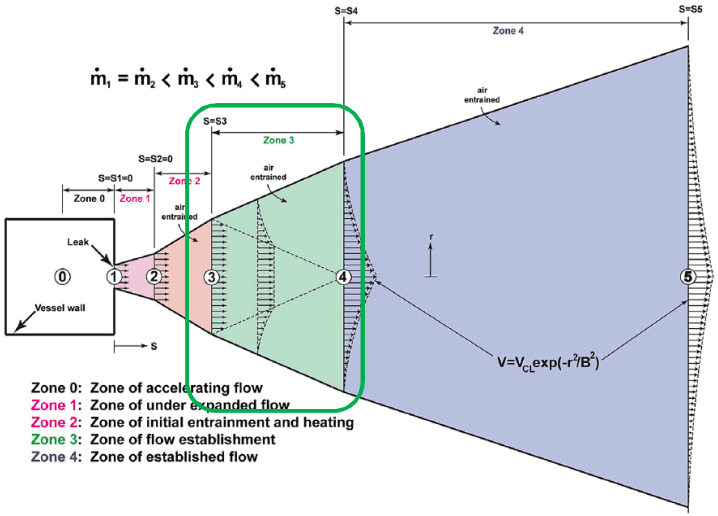

unknowns
assumed value

$$V_{CL,4} = V_3$$

Mass

$$\rho_3 \frac{D_3^2}{4} = B_4^2 \left[\rho_{amb} - \frac{\lambda^2}{\lambda^2+1}(\rho_{amb} - \rho_{CL,4})\right]$$

Momentum

$$\underbrace{(\rho_{amb} - \rho_3)\frac{D_3^2}{4}}_{S_3} = \underbrace{B_4^2 \left[\frac{\rho_{amb}}{2} - \frac{\lambda^2}{2\lambda^2+1}(\rho_{amb} - \rho_{CL,4})\right]}_{S_4}$$

Winters, SAND Report 2009-0035

Zone 4 modeled with previous SNL 1D integral jet/plume models that invoke self-similarity – FY08.

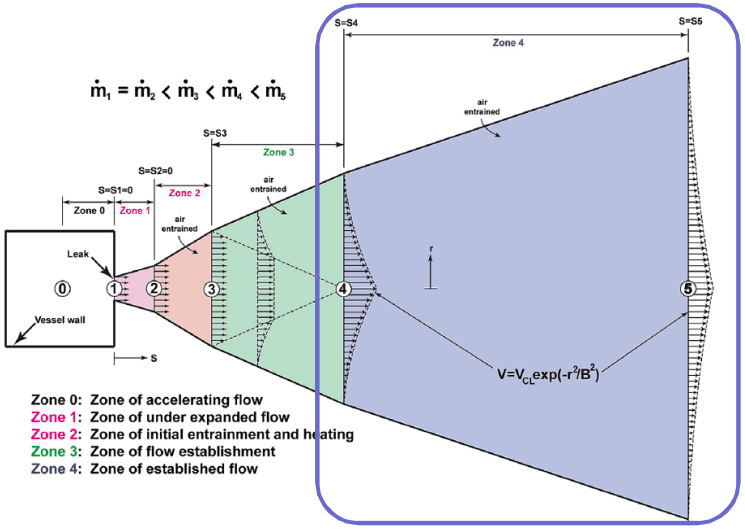

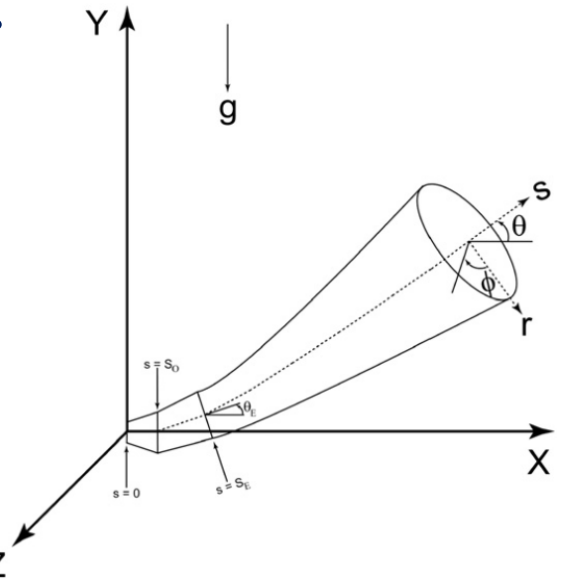

Houf & Schefer, IJHE, 2008

Mass $$\frac{\partial}{\partial S}\int_0^{2\pi}\int_0^{\infty}\rho V r dr d\phi = \rho_{amb} E$$

x-Mom $$\frac{\partial}{\partial S}\int_0^{2\pi}\int_0^{\infty}\rho V^2 \cos\theta\, r dr d\phi = 0$$

y-Mom $$\frac{\partial}{\partial S}\int_0^{2\pi}\int_0^{\infty}\rho V^2 \sin\theta\, r dr d\phi = \int_0^{2\pi}\int_0^{\infty}(\rho_{amb}-\rho) g r dr d\phi$$

Species $$\frac{\partial}{\partial S}\int_0^{2\pi}\int_0^{\infty}\rho V Y r dr d\phi = 0$$

Energy $$\frac{\partial}{\partial S}\int_0^{2\pi}\int_0^{\infty}\rho V (h-h_{amb}) r dr d\phi = 0$$

Zone 4 modeled using previously developed SNL integral jet/plume models – FY08

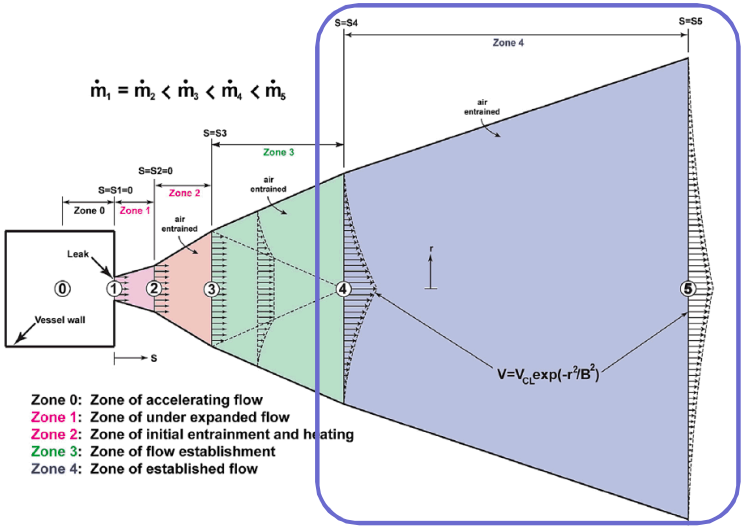

Entrainment modeled to include buoyancy & momentum effects

- F_{rL}: Jet Froude length
- α_b: Buoyancy entrainment coefficient
- α_m: Momentum entrainment coefficient
- g: Gravity constant

$$E_{mom} = \alpha_m \left(\frac{\pi D^2}{4}\frac{\rho V^2}{\rho_{amb}}\right)^{\frac{1}{2}}$$

$$E_{buoy} = \frac{\alpha_b}{F_{r_L}}(2\pi V_{CL} B)\sin\theta$$

$$F_{r_L} = \frac{V_{CL}^2 \rho_{exit}}{gB(\rho_{amb} - \rho_{CL})}$$

Houf & Schefer, IJHE, 2008

Mass
$$\frac{d}{dS}\left\{V_{CL}B^2\left[\rho_{amb} - \frac{\lambda^2}{\lambda^2+1}(\rho_{amb}-\rho_{CL})\right]\right\} = \frac{\rho_{amb}(E_{mom}+E_{buoy})}{\pi}$$

x-Mom
$$\frac{d}{dS}\left\{V_{CL}^2B^2\cos\theta\left[\rho_{amb} - \frac{2\lambda^2}{2\lambda^2+1}(\rho_{amb}-\rho_{CL})\right]\right\} = 0$$

y-Mom
$$\frac{d}{dS}\left\{V_{CL}^2B^2\sin\theta\left[\frac{\rho_{amb}}{2} - \frac{\lambda^2}{2\lambda^2+1}(\rho_{amb}-\rho_{CL})\right]\right\} = (\rho_{amb}-\rho_{CL})\lambda^2 B^2$$

Species
$$\frac{d}{dS}\{V_{CL}B^2(\rho_{amb}Y_{amb} - \rho_{CL}Y_{CL})\} = 0$$

Energy
$$\frac{\partial}{\partial S}\left\{\int_0^\infty \rho V[h(P_{amb},\rho) - h_{amb}(P_{amb},\rho_{amb})]r\,dr\right\} = 0$$

Solution possible via commonly available 1D ODE solvers.

Model results compare favorably to experiments from Karlsruhe Institute of Technology.

Case	Reservoir pressure [MPa]	Reservoir temperature [K]	Leak diameter [mm]
1	1.7	298	2
2	6.85	298	1
3	0.825	80	2
4	3.2	80	1

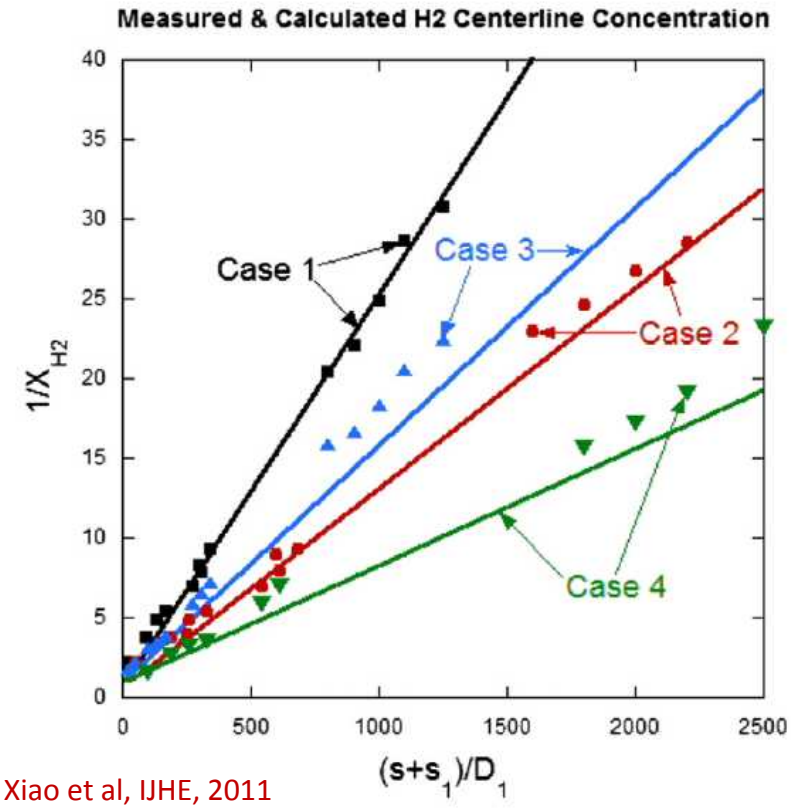

Xiao et al, IJHE, 2011
Houf & Winters, IJHE, 2013

However, no well-controlled validation data is available at lower temperatures where multi-phase flows are expected (i.e., T < 77 K).

Multi-phase behavior—particularly for high-humidity conditions—is important.

Liquid and vapor phases have different velocities due to density differences — slip models have captured these effects in CFD simulations.

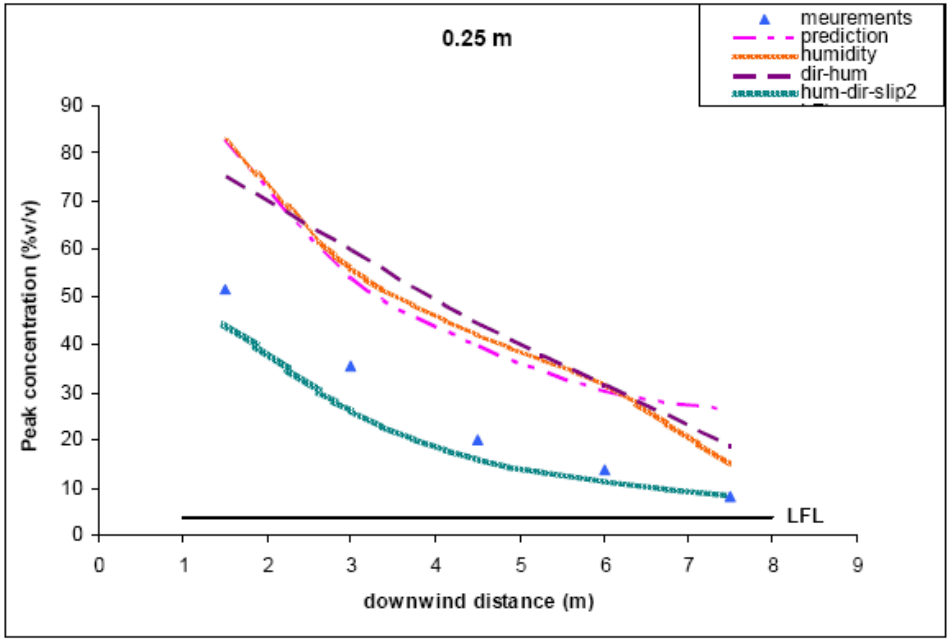

HSL Measurements: Sample probes

Hooker et al, ICHS, 2011

ADREA-HF CFD Simulations

Giannissi et al, ICHS, 2013

Substantial differences in model results suggest 2-phase effects cannot be neglected for LH2 releases

Experiments had poor control of release and environmental boundary conditions, which are needed for suitable benchmark data.

Proposal is to build an LH2 delivery system that can be integrated w/ existing SNL laboratory infrastructure.

Delivery system would generate ultra-cold vapor and liquid H2 jets

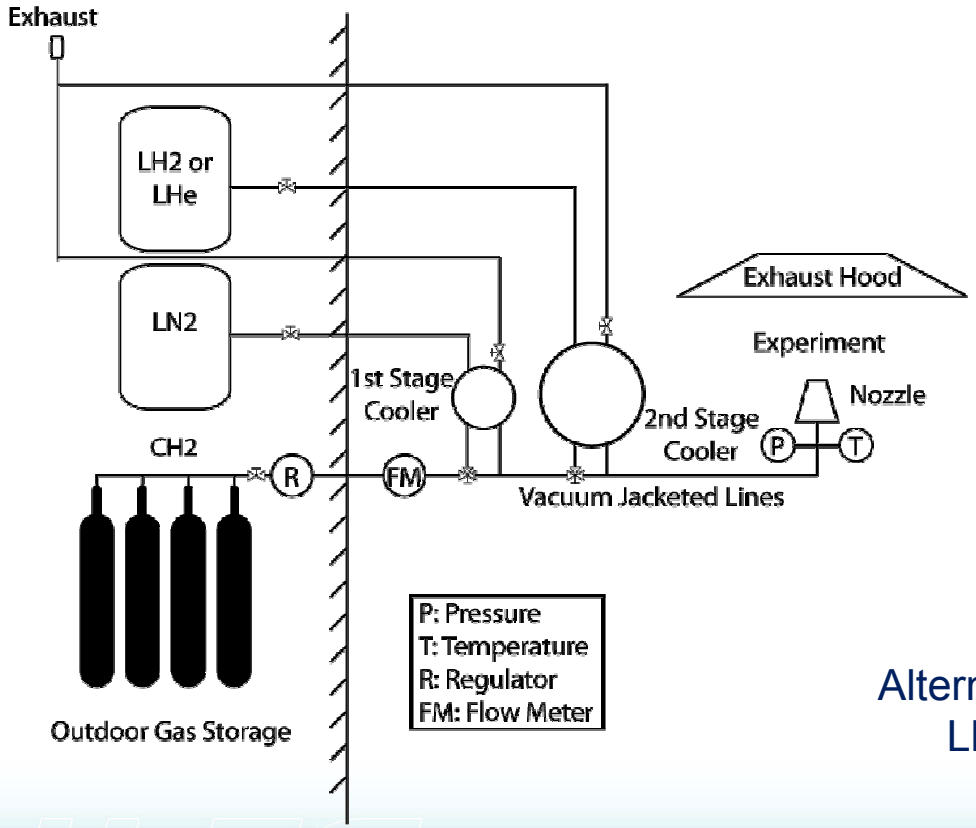

LH2 or LHe generation via a commercial cryo-refrigerator

Alternatively, LH2 could be transported from LLNL to SNL from an available LH2 tank

System design, construction, & verification ~12 months, w/ another 6-12 months for measurements – system cost ~$150K plus labor.

Scalar field to be measured via Rayleigh scatter imaging in established flow zone to validate LH2 release model.

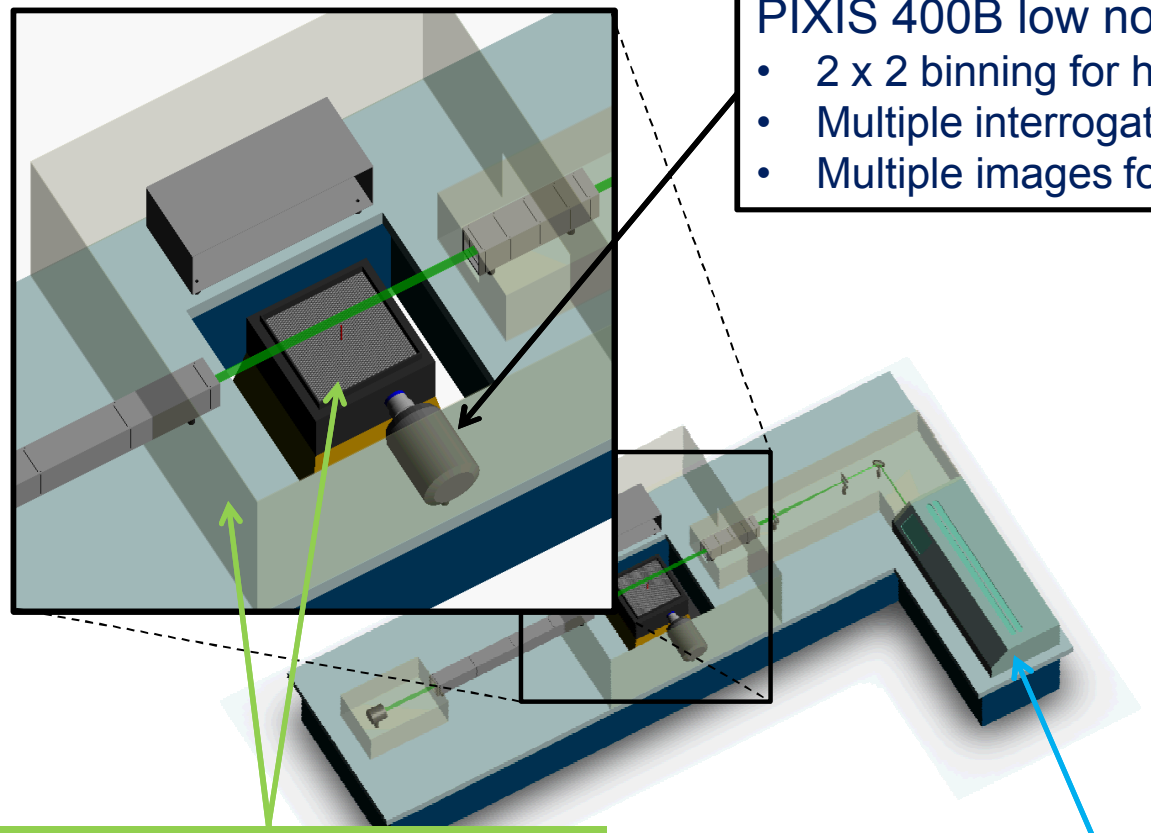

PIXIS 400B low noise CCD Camera

- 2 x 2 binning for high signal-to-noise (~400:1)
- Multiple interrogation regions to image full jet
- Multiple images for converged statistics

Air co-flow & barriers to minimize impact of room currents

Nd:YAG injection seeded laser (1 J/pulse @ 532 nm)

Opportunity for additional upstream measurements using complementary Raman diagnostics in an adjacent lab.

SNL Behavior Modeling — Research path & planned LH2 Experiments

Isaac Ekoto
Ethan Hecht
Chris San Marchi

Sandia National Laboratories is a multi-program laboratory managed and operated by Sandia Corporation, a wholly owned subsidiary of Lockheed Martin Corporation, for the U.S. Department of Energy's National Nuclear Security Administration under contract DE-AC04-94AL85000. SAND NO. 2011-XXXXP

Backup Slides

Jet Flame Radiation Modeling

Three jet flame radiative heat flux model categories:

Single Point Source (SPS) models

Flame shape:
- Non-dimensional radiant power to estimate radiant load distribution

Radiant fraction models:
- Empirical function: temperature, composition, release rate, soot, residence time, heat release

Sivathanu & Gore, Combust Flame, 1993
Molina et al., Proc Combust Inst, 2007

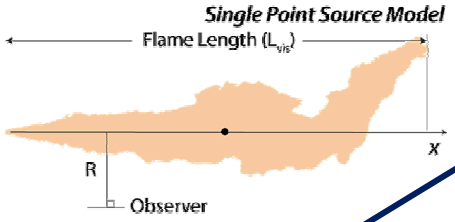

Single Surface models

Flame shape:
- Assumed flame shape (e.g., cone) w/ empirically tuned radiating surface
- Geometric View Factors to calculate radiation transfer
- Empirical wind/buoyancy corrections

Chamberlain, Chem Eng Res Des, 1987
Johnson et al., Process Safety Environ Prot, 1994

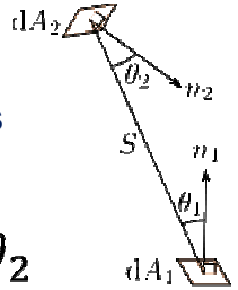

$$VF_{1\to 2} = \frac{\cos\theta_1 \cos\theta_2}{\pi S^2}$$

Radiant fraction models:
- Empirical function of exit velocity

Multi Source Models (MSM)

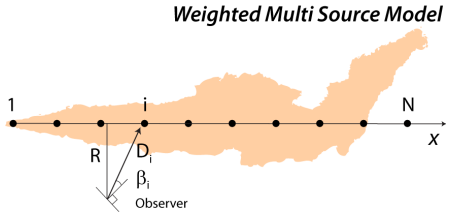

Flame shape:
- Weighted source emitters along flame centerline

Radiant fraction models:
- Same as SPS models

De-Faveri et al., Hydrocarbon Processing, 1985
Hankinson & Lowesmith, Combust Flame, 2012

Previous Accomplishments

Large-scale flame data supplied by Air Products and Chemicals Inc.

d_j [mm]	[kg/s]	L_{vis} [m]	p_0 [barg]	T_0 [K]	T_{amb} [K]	p_{amb} [bar]
50.8	7.4	48.5	62.1	288	280	1.01

Single Point Source Model

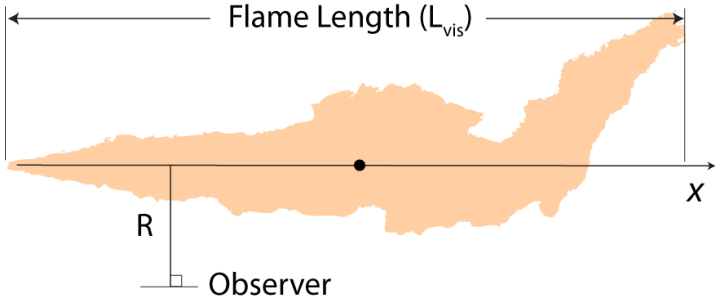

Old model used to inform NFPA 2/55

Weighted Multi Source Model

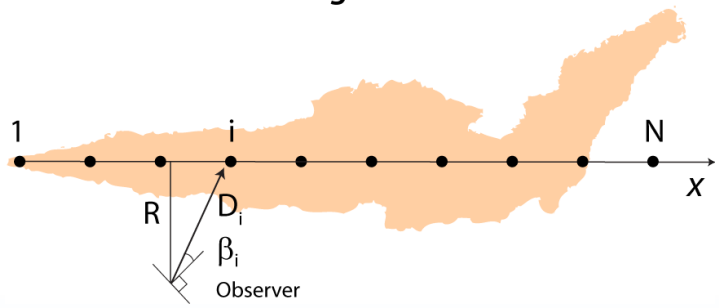

Houf and Schefer, IJHE, 2007

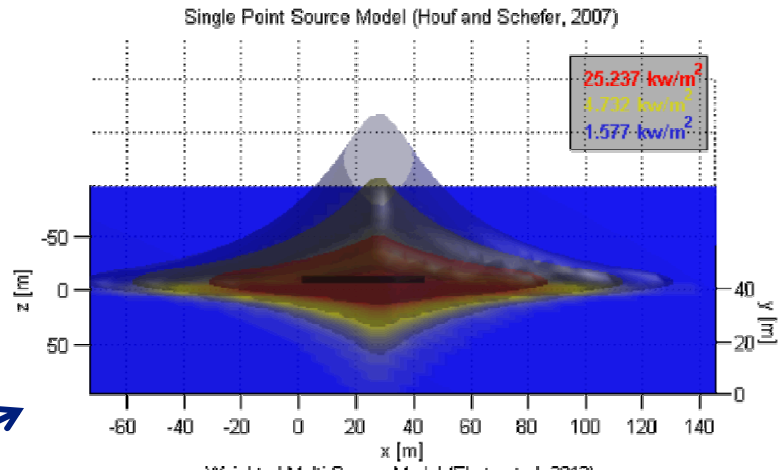

Ekoto et al., Proc IPC, 2012

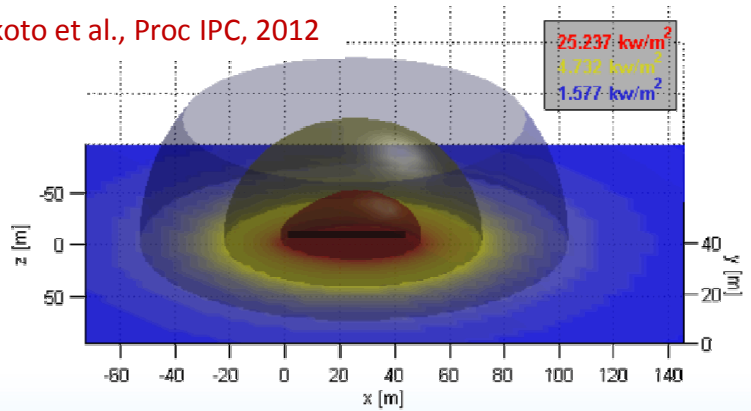

Improved radiative heat flux boundaries for more accurate harm & improved recommendations for reduced separation distances.

- **Model can be improved with a better prediction of flame trajectory to better**

Flame integral model is similar to 1D jet integral models

Cheng et al, Combust Flame, 1992

H2 jet flame
Re = 13,600

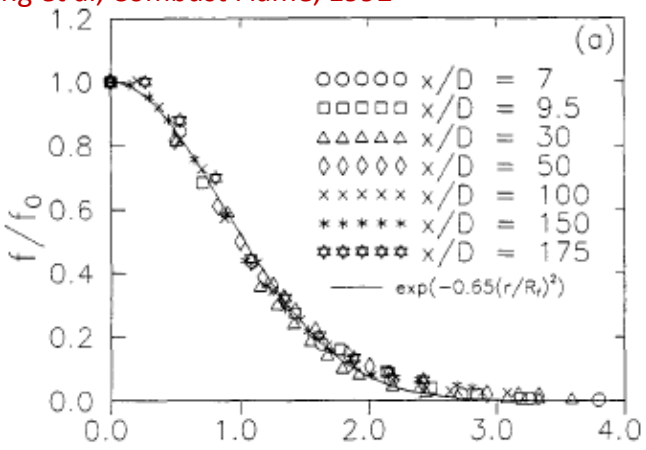

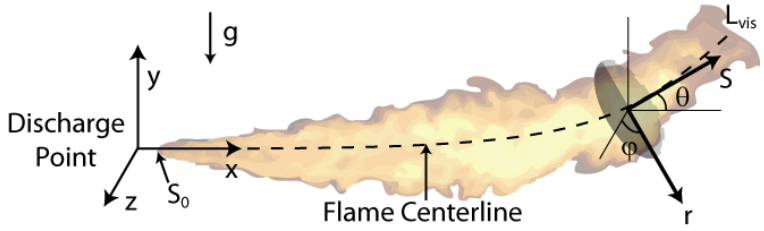

Species are no longer conserved & excess state variable profiles depend on the degree of chemical reaction

Self-similar, Gaussian mixture fraction profiles observed at all radials throughout the flame

$$\frac{\partial}{\partial S}\int_0^{2\pi}\int_0^{\infty}\rho VYr\,dr\,d\phi$$ replaced by, $$\frac{d}{dS}\int_0^{2\pi}\int_0^{\infty}\rho Vfr\,dr\,d\phi = 0$$ where, $$f = Y_{H_2} + Y_{H_2O}\frac{MW_{H_2}}{MW_{H_2O}}$$

H_2 Species Conservation

Mixture Fraction Conservation

Mixture fraction is a conserved scalar that can replace H_2 mass fraction in the conservation equations

Flame integral model is similar to existing 1D jet models

Cheng et al, Combust Flame, 1992

H2 jet flame
Re = 13,600

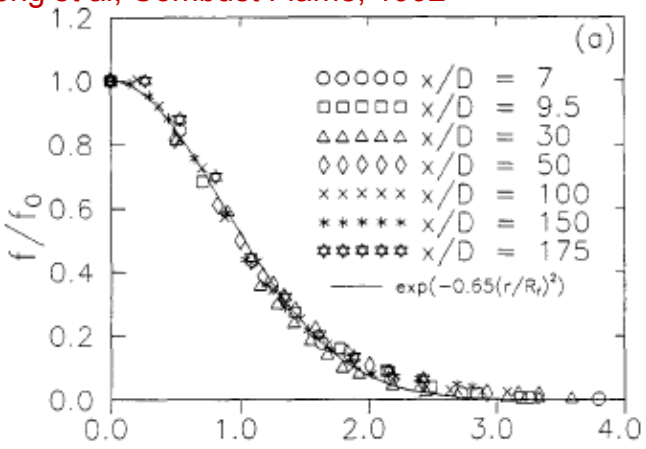

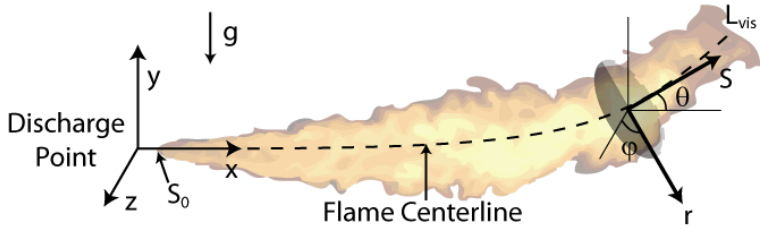

Species are no longer conserved & **excess state variable profiles depend on the degree of chemical reaction**

Self-similar, Gaussian mixture fraction profiles observed at all radials throughout the flame

Barlow & Carter, Combust Flame, 1994

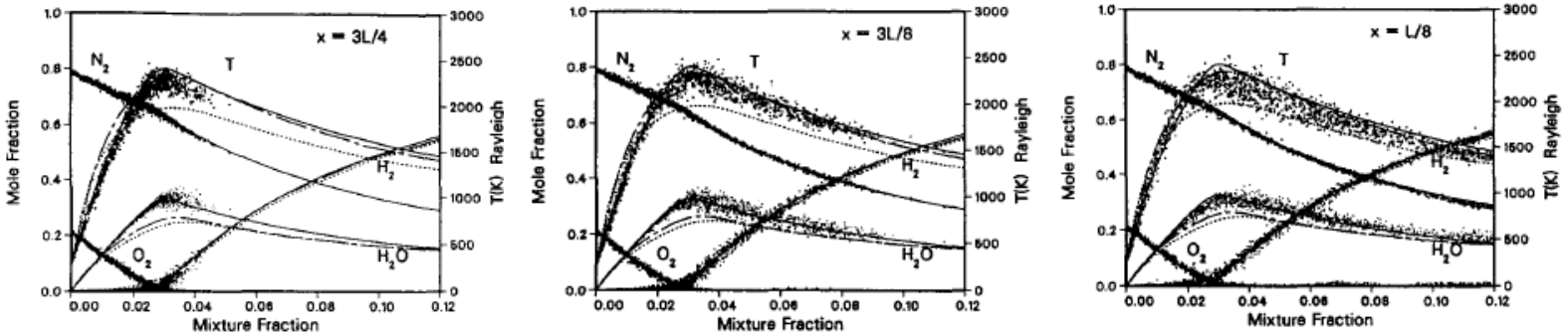

H2 jet flame; Re = 10,000

Composition/Temperature at most points was close to equilibrium solution — energy conservation can be neglected if equilibrium kinetics are assumed

Model performs well when applied to large-scale flames

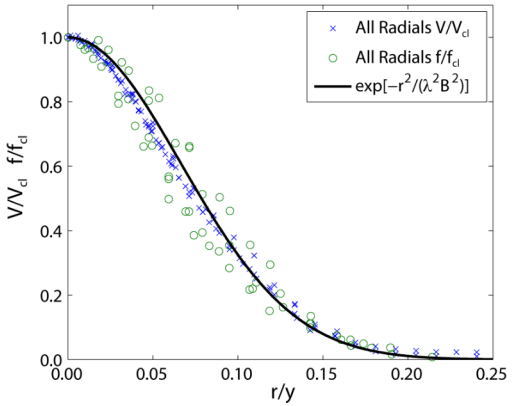

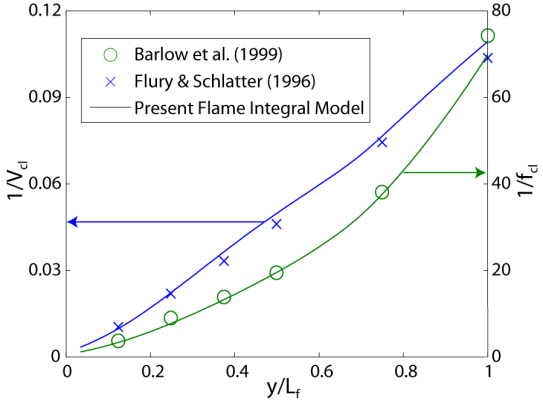

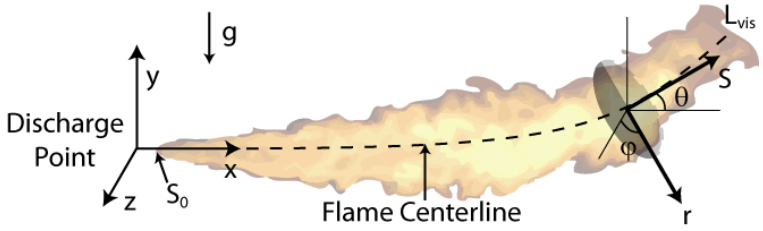

Entrainment rate coefficients & jet spreading ratios adjusted to match experimental data

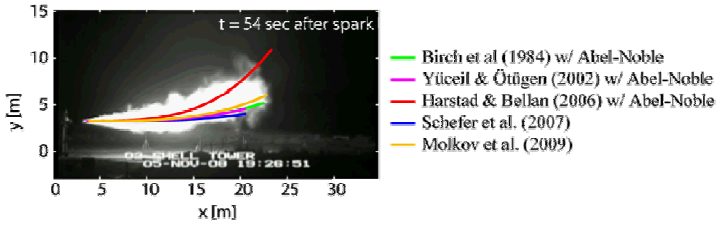

Centerline trajectory results highly dependent on choked source model

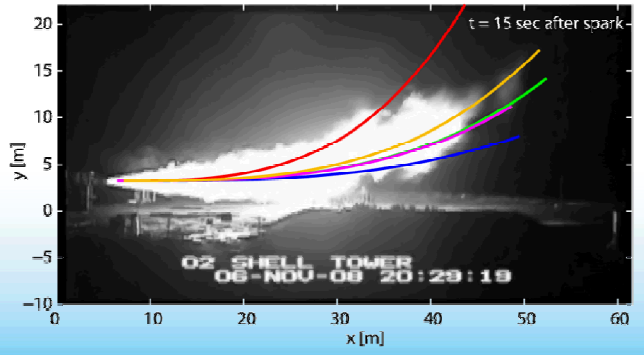

Ekoto et al., IJHE, (Under Review)

Integral flame model developed to improve downstream H2 jet flame heat flux prediction.

Ekoto et al. ICHS 2013

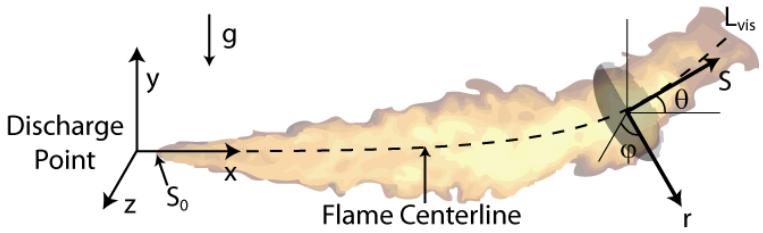

d_j [mm]	$\dot{m}$ [kg/s]	p_0 [barg]	T_0 [K]	RH [%]	T_{amb} [K]	p_{amb} [mbar]	U_{wind} [m/s]	Wind dir [°]
52.5	7.4	62.1	287.8	94.5	280	1011	0.83	34.0

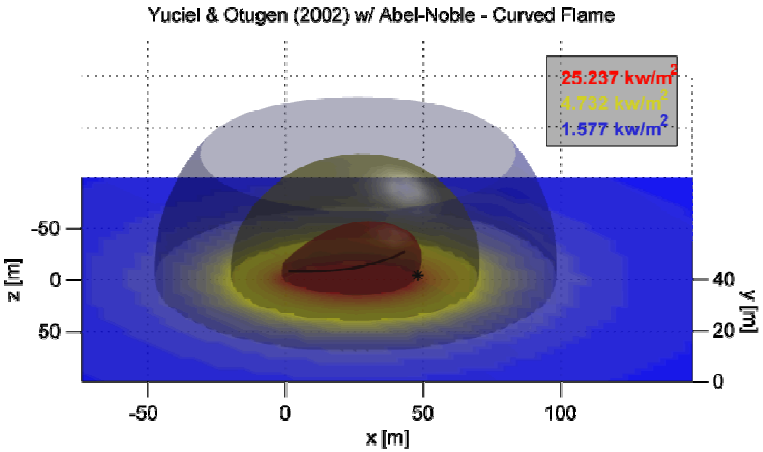

Adjusts placement of radiative emitters for new multi-source model – FY12 accomplishment

Notional Nozzle Model	L_f [m]	q_{rad} (Straight) [kW/m²]	q_{rad} (Curved) [kW/m²]
Measurement	45.9	–	23.9
Birch et al. (1984) w/ Abel-Noble	49.3	97.3	29.9
Yüceil & Ötügen (2002) w/ Abel-Noble	44.6	34.8	23.8
Schefer et al. (2007)	44.6	34.8	28.1
Harstad & Bellan (2006) w/ Abel-Noble	52.7	189.8	13.2
Molkov et al. (2009)	49.9	113.2	25.6

SNL preferred source model →

Similar wind corrections in progress

Slot Nozzle Modeling

Unchoked slot jets have been thoroughly investigated

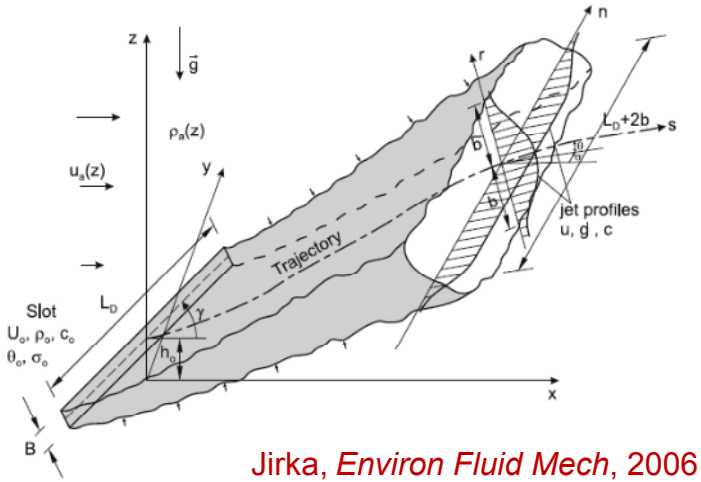

Jirka, *Environ Fluid Mech*, 2006

Planar jet integral model has been developed

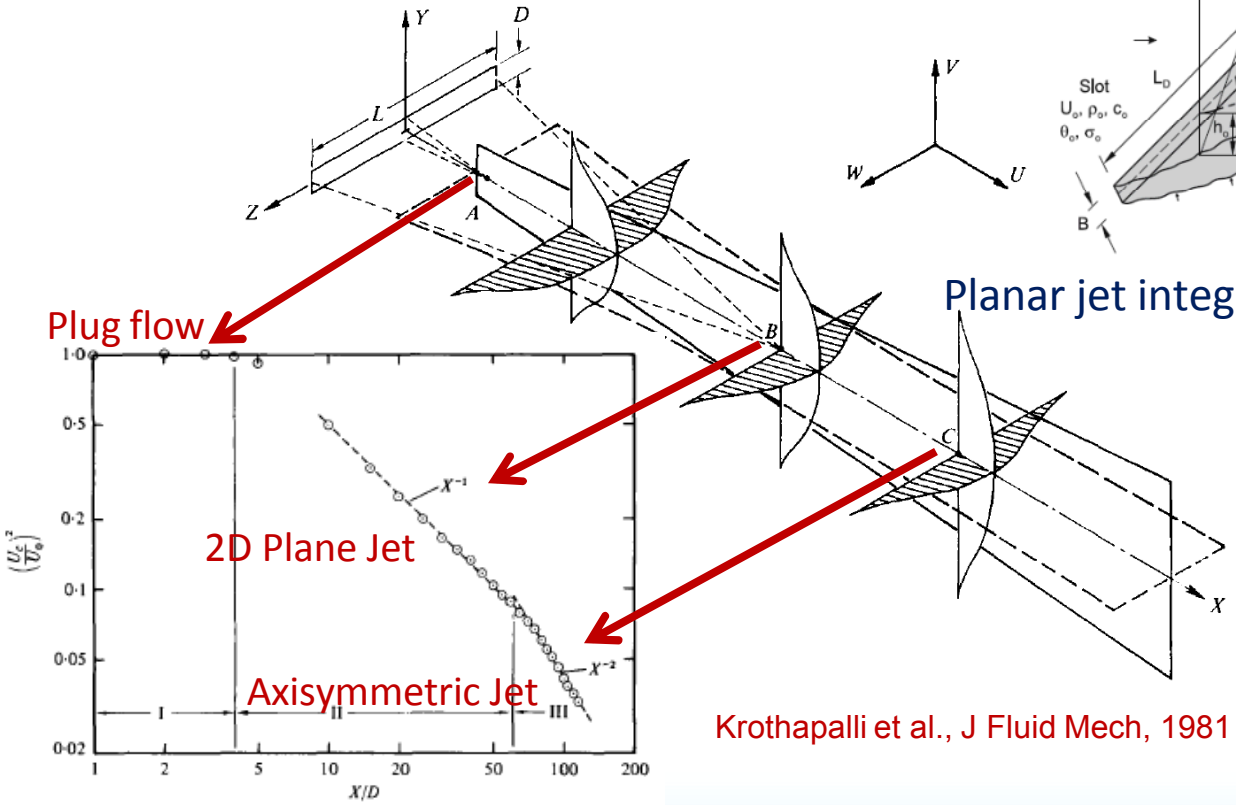

Krothapalli et al., J Fluid Mech, 1981

Distinct 2D region with inverse ½ power centerline decay rate exists

Unclear if models are applicable to choked slot jets

Close-up schlieren imaging reveals unique slot nozzle behavior – FY13

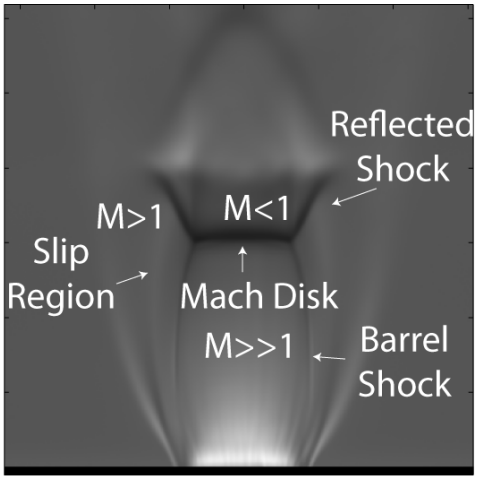

Strong, sharply converging incident corner shock is missing from the minor axis plane

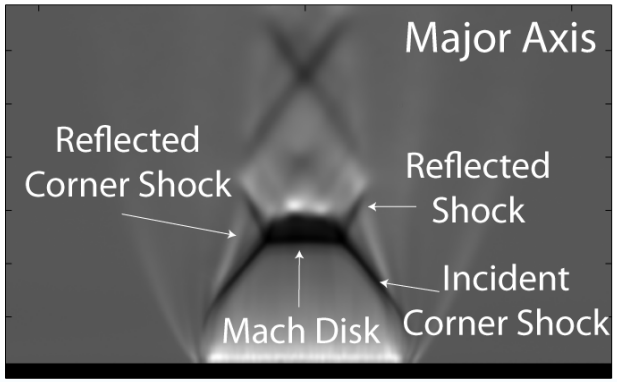

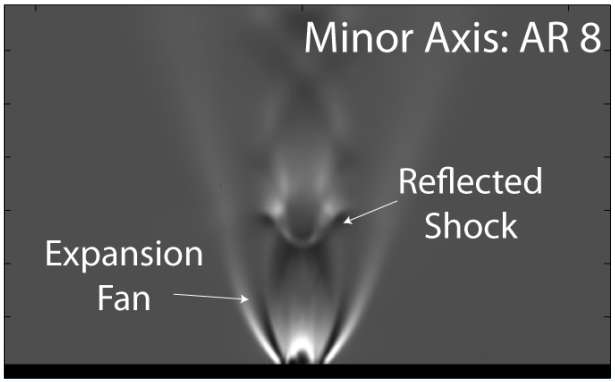

Unclear if existing choked flows notional nozzle models predict correct effective diameters and densities

Mean mass fraction slot jet contours confirm axis switching in the scalar field

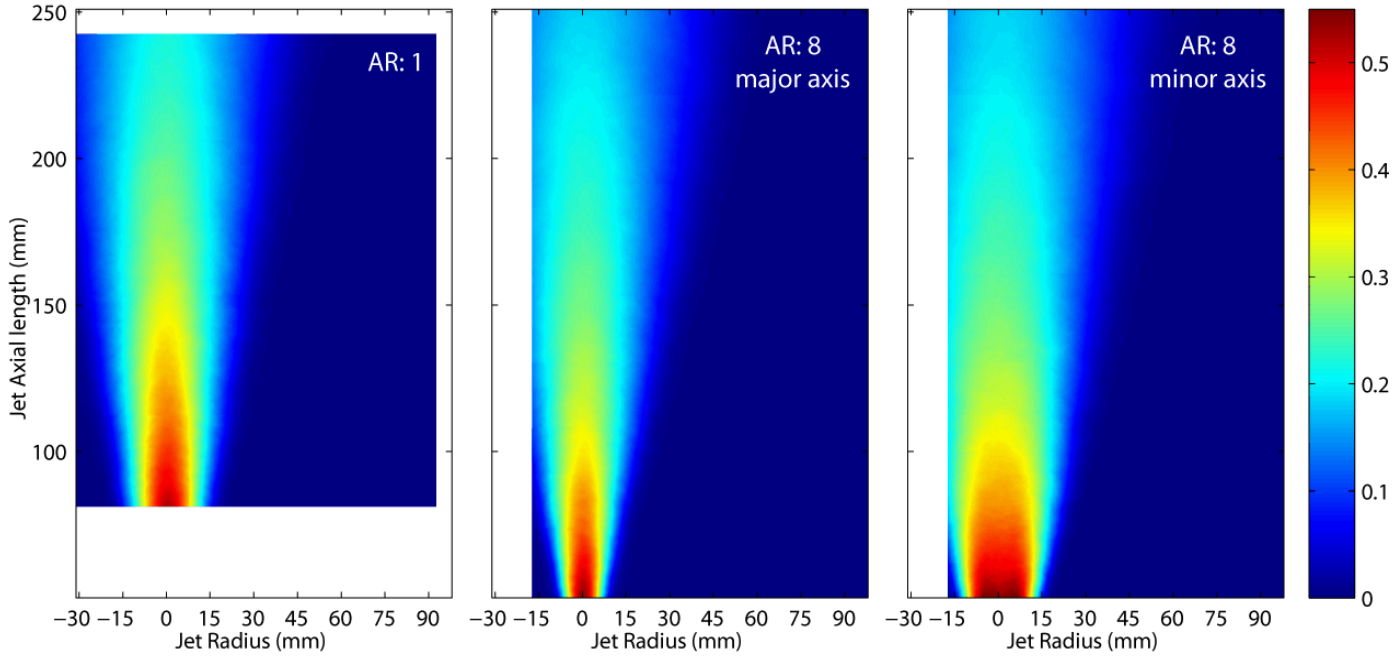

Elevated downstream mass fraction contours for the axisymmetric jet

D_{eq} = 1.5 mm
p_0 = 10 bar

Concentration decay rates remained relatively linear throughout the measurement region

Planar decay region (half-power) not observed

- Upstream of interrogation region?

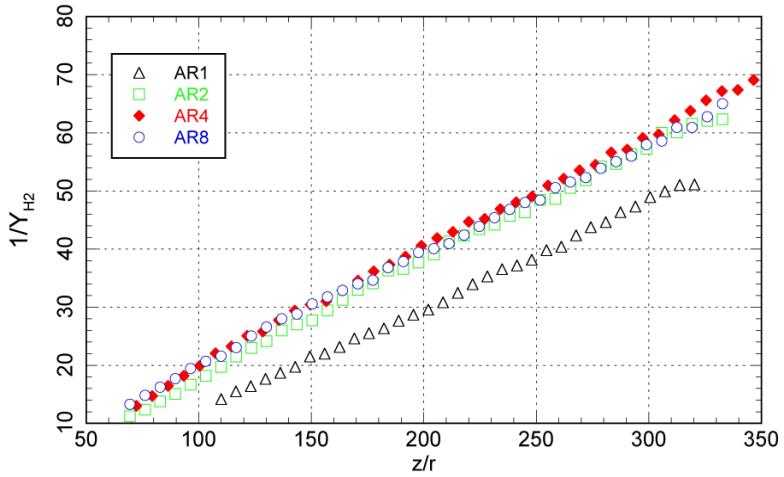

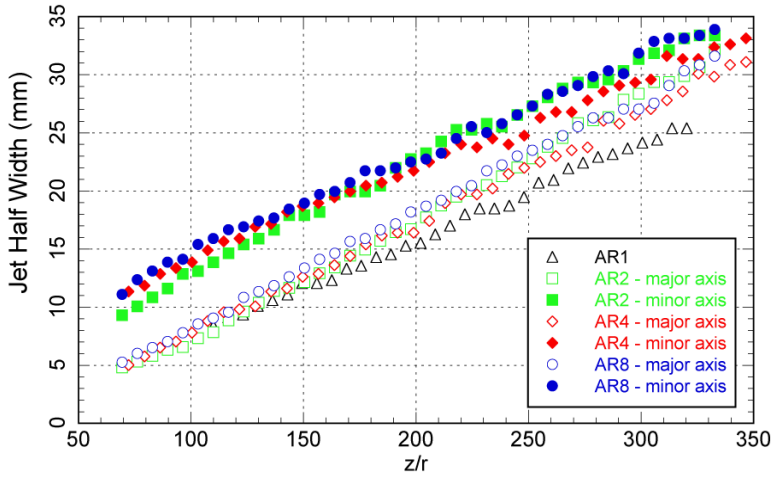

Major & minor axis jet half widths appear to converge

- Half widths larger than for corresponding axisymmetric jet
- Slightly non-linear growth rates – unclear when convergence occurs

Normalized concentration radial profiles along the major/minor axes do not collapse

Axisymmetric profiles collapsed to uniform curves as expected

Normalized profiles grew ***wider along the major axis*** and ***narrower along the minor axis***

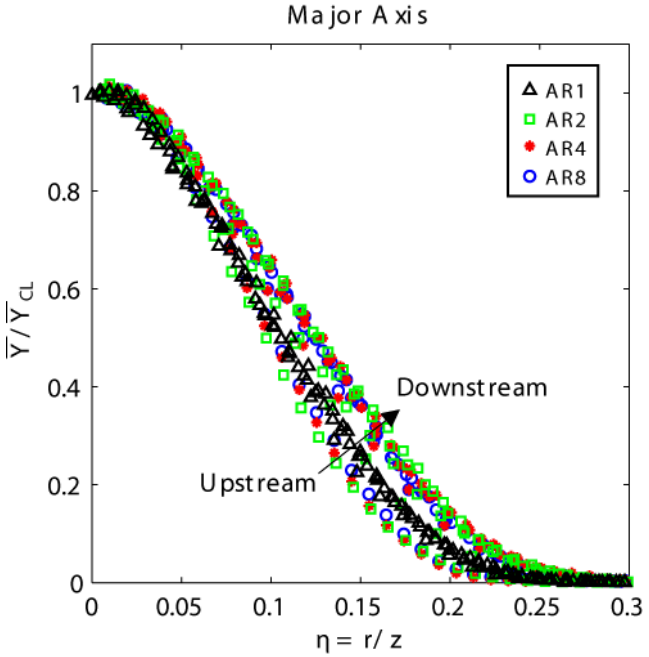

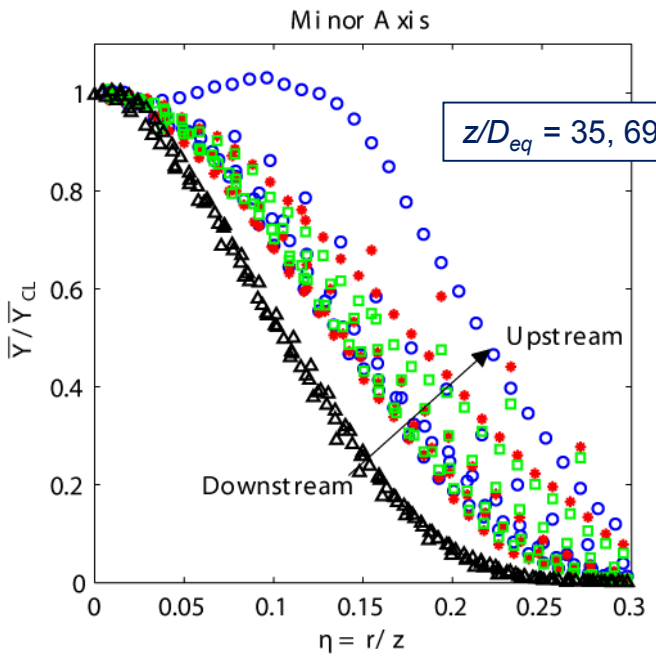

Minor axis peak H_2 ***near-field*** concentrations observed away from the centerline – not predicted by planar integral models

These data will be used to refine jet release characteristics for different release morphologies